UDP-3-*O*-(*R*-3-Hydroxymyristoyl)-*N*-acetylglucosamine Deacetylase of *Escherichia coli* Is a Zinc Metalloenzyme†

Jane E. Jackman, Christian R. H. Raetz, and Carol A. Fierke*

Department of Biochemistry, Duke University Medical Center, Box 3711, Durham, North Carolina 27710

Received September 30, 1998; Revised Manuscript Received December 3, 1998

ABSTRACT: The enzyme UDP-3-*O*-(*R*-3-hydroxymyristoyl)-GlcNAc deacetylase (LpxC) catalyzes the committed step in the biosynthesis of lipid A and is therefore a potential antibiotic target. Inhibition of this enzyme by hydroxamate compounds [Onishi, H. R.; Pelak, B. A.; Gerckens, L. S.; Silver, L. L.; Kahan, F. M.; Chen, M. H.; Patchett, A. A.; Stachula, S. S.; Anderson, M. S.; Raetz, C. R. H. (1996) *Science 274*, 980−982] suggested the presence of a metal ion cofactor. We have investigated the substrate specificity and metal dependence of the deacetylase using spectroscopic and kinetic analyses. Comparison of the steady-state kinetic parameters for the physiological substrate UDP-3-*O*-(*R*-3-hydroxymyristoyl)-GlcNAc and an alternative substrate, UDP-GlcNAc, demonstrates that the ester-linked *R*-3-hydroxymyristoyl chain increases k_{cat}/K_M (5×10^6)-fold. Metal-chelating reagents, such as dipicolinic acid (DPA) and ethylenediaminetetraacetic acid, completely inhibit LpxC activity, implicating an essential metal ion. Plasma emission spectroscopy and colorimetric assays directly demonstrate that purified LpxC contains bound Zn^{2+}. This Zn^{2+} can be removed by incubation with DPA, causing a decrease in the LpxC activity that can be restored by subsequent addition of Zn^{2+}. However, high concentrations of Zn^{2+} also inhibit LpxC. Addition of Co^{2+}, Ni^{2+}, or Mn^{2+} to apo-LpxC also activates the enzyme to varying degrees while no additional activity is observed upon the addition of Cd^{2+}, Ca^{2+}, Mg^{2+}, or Cu^{2+}. This is consistent with the profile of metals that substitute for catalytic zinc ions in metalloproteinases. Co^{2+} ions stimulate LpxC activity maximally at a stoichiometry of 1:1. These data demonstrate that *E. coli* LpxC is a metalloenzyme that requires bound Zn^{2+} for optimal activity.

The outer leaflet of the outer membranes of Gram-negative bacteria contains a unique molecule known as lipopolysaccharide (LPS).[1] LPS renders Gram-negative bacteria impermeable to certain antibiotics and bactericidal compounds. The lipid A portion of LPS causes many of the toxic side effects associated with Gram-negative bacterial infections (*1*). Lipid A from the Gram-negative bacteria *Escherichia coli* is a hexa-acylated disaccharide of glucosamine sugars bearing phosphate residues at positions 1 and 4′, and is essential for bacterial growth (*2*). Inhibition of lipid A biosynthesis not only kills bacteria but also increases the sensitivity of bacteria to certain antibiotics, such as erythromycin, that are normally excluded by the outer membrane (*3*).

The identification of the enzymes responsible for biosynthesis of lipid A has provided new targets in the search for antibacterial agents (*1*, *2*). The recent description of bactericidal compounds that inhibit the second enzyme in the *E. coli* lipid A pathway demonstrates the feasibility of this approach (*4*). The target enzyme UDP-3-*O*-(*R*-3-hydroxymyristoyl)-*N*-acetylglucosamine deacetylase (LpxC) removes an acetyl moiety from the 2-N position of glucosamine in the lipid A precursor UDP-3-*O*-(*R*-3-hydroxymyristoyl)-*N*-acetylglucosamine (UDP-3-*O*-acyl-GlcNAc) (Figure 1). A second *R*-3-hydroxymyristoyl acyl group is then added to the deacetylated product in a reaction catalyzed by LpxD (*5*, *6*). Due to the thermodynamically unfavorable nature of the reaction catalyzed by the first enzyme in the lipid A biosynthetic pathway, LpxA, the LpxC reaction is the committed step for the biosynthesis of lipid A (*7*).

The LpxC inhibitors described by Onishi and co-workers (4) require a hydroxamic acid functional group for effective inhibition (Figure 1). Hydroxamate-containing compounds are often potent inhibitors of Zn^{2+} metalloamidases, including thermolysin and angiotensin converting enzyme (*8*, *9*). Crystallographic studies of hydroxamate inhibitors bound to thermolysin demonstrate that the hydroxamic acid functional group decreases catalytic activity by coordinating the catalytically important zinc ion (*10*, *11*). Hydroxamate inhibitors of LpxC may similarly interact with an active site zinc ion. Consistent with this hypothesis, previous studies have demonstrated that LpxC from *Pseudomonas aeruginosa* is

† This work was supported by the National Institutes of Health (GM40602 to C.A.F. and GM51310 to C.R.H.R.). J.E.J. is supported in part by a National Science Foundation Predoctoral Fellowship (DGE092-53851).

* To whom correspondence should be addressed.

[1] Abbreviations: BSA, bovine serum albumin: bis-tris, [bis(2-hydroxyethyl)amino-tris(hydroxymethyl)methane; DPA, dipicolinic acid; DTT, dithiothreitol; EDTA, ethylenediaminetetraacetic acid; HEPES, *N*-(2-hydroxyethyl)piperazine-*N*′-2-ethanesulfonic acid; ICP, inductively coupled plasma emission spectroscopy; LPS, lipopolysaccharide; LpxC, UDP-3-*O*-(*R*-3-hydroxymyristoyl)-*N*-acetylglucosamine deacetylase; PAR, 4-(2-pyridylazo)resorcinol; TCEP, tris(2-carboxyethyl)phosphine; UDP-3-*O*-acyl-GlcNAc, uridine 5′-diphospho-3-*O*-(*R*-3-hydroxymyristoyl)-*N*-acetylglucosamine; UDP-GlcNAc, uridine 5′-diphospho-*N*-acetylglucosamine.

10.1021/bi982339s CCC: $18.00
Published on Web 01/22/1999

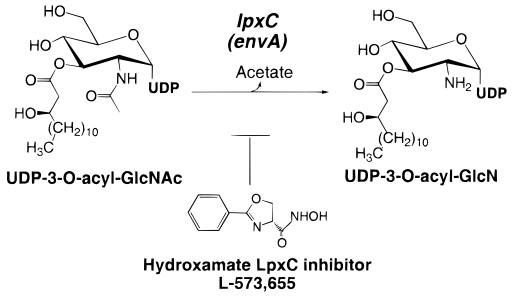

FIGURE 1: Reaction catalyzed by *E. coli* LpxC. An inhibitory hydroxamate compound (L-573,655) described by Onishi and coworkers (4) is shown here.

inhibited by ethylenediaminetetraacetic acid (EDTA), and deacetylase activity can be restored by the addition of transition metals to crude cell extracts (*12*), suggesting the presence of a catalytically important metal ion. Similar experiments with cell extracts containing a mutant form of the *E. coli* LpxC (*12*) suggest that this protein may also be a metalloenzyme. However, no definitive metal analyses have been performed to demonstrate directly the presence of a metal ion cofactor in the purified LpxC protein.

Zinc-containing metalloenzymes have been extensively studied, and examples of enzymes that contain zinc ions can be found in each one of the six classes of enzymes (*13*). The roles that zinc ions play in catalysis are varied; however, a single essential zinc ion can usually be categorized as either structural or catalytic. In this work, we characterize the metal ion requirement of LpxC from *E. coli*. We demonstrate that LpxC contains Zn^{2+} that is required for maximal activity. This Zn^{2+} can only be substituted by Co^{2+} and Ni^{2+}, and to a lesser extent, Mn^{2+}. Additionally, metal chelators such as EDTA and dipicolinic acid (DPA) as well as high concentrations of Zn^{2+} inhibit LpxC activity. These data indicate that the bound Zn^{2+} in LpxC is essential for catalytic activity. Furthermore, the metal ion dependence and inhibition of LpxC is very similar to that previously observed for other metalloproteinases (*14*, *15*), suggesting that the zinc ion in this deacetylase may play a catalytic role. However, no known Zn^{2+} binding motifs have been identified in the LpxC sequence, suggesting that this enzyme may be a member of a novel class of Zn^{2+}-containing deacetylases.

MATERIALS AND METHODS

Materials. [α-^{32}P]UTP was purchased from NEN Dupont. PEI−cellulose TLC plates were obtained from E. Merck, Darmstadt, Germany. EDTA, bis-tris buffer, and HEPES buffer were purchased from Sigma as Ultrapure reagents. Bovine serum albumin (BSA), essentially fatty acid free, was purchased from Sigma. $ZnSO_4$ volumetric standard solution (0.0499 M) and Zn^{2+} AA/ICP calibration/check standard were purchased from Aldrich.

Enzyme Induction and Purification. A plasmid containing the cloned *E. coli* lpxC gene under control of a T7 RNA polymerase promoter (pET11a-EnvA) was a generous gift from Dr. Matt Anderson, Merck and Co. Inc., Rahway, NJ (*6*). Growth and induction of LpxC from this plasmid were performed essentially as previously reported (*6*), with minor variations. BL21(DE3)pLysS cells (*16*) were transformed with pET11a-EnvA and grown at 34 °C in rich induction medium (*17*) to $A_{620} = 0.5$. Expression from the *lpxC* gene was induced by the addition of 1 mM isopropyl D-thiogalactopyranoside and 0.1 mM $ZnSO_4$. After 6 h, the cells were harvested and resuspended in 10 mM HEPES, pH 7, containing 100 μM $ZnSO_4$ and 2 mM dithiothreitol (DTT), to 4 times the volume of the wet cell paste and then frozen at −80 °C. Lysis of the cells with detergent and purification of the deacetylase by ammonium sulfate precipitation followed by anion exchange chromatography in the absence of detergent were carried out as described by Young and colleagues (*6*). The final deacetylase protein was more than 95% pure as determined by SDS−PAGE (*18*). Electrospray mass spectrometry demonstrated that the purified protein was homogeneous, with a molecular mass of 33 960 ± 10, in agreement with the predicted molecular mass of 33 956 with the N-terminal f-Met intact. Accurate measurement of the protein concentration is crucial for the determination of kinetic parameters and the stoichiometry of metal binding. LpxC exhibits anomalously high affinity for Coomassie dye, precluding the use of colorimetric methods to determine accurate protein concentrations. Therefore, the extinction coefficient at 280 nm of the purified protein was determined by dry weight analysis to be 24 500 M^{-1} cm^{-1}.

Metal Analysis. Metal analyses were performed by two independent methods. Inductively coupled plasma emission spectroscopy (ICP) was performed at Garratt-Callahan Co., Millbrae, CA. Each LpxC sample, including a buffer reference sample, was analyzed for the presence of the following 23 elements: Al, Ba, Be, Cd, Ca, Cr, Co, Cu, Fe, Pb, Li, Mg, Mn, Mo, Ni, K, Si, Ag, Na, Sr, Sn, V, and Zn. Zinc standard solutions were analyzed simultaneously to ensure the accuracy of this method. Samples contained >10 μM Zn^{2+}-reconstituted LpxC or >50 μM apo-LpxC to analyze Zn^{2+} concentrations significantly above any background contamination. A colorimetric assay based on the absorbance of the metal-chelating reagent 4-(2-pyridylazo)-resorcinol (PAR) was also used to measure Zn^{2+} concentrations (*19*, *20*). In this assay, LpxC (2−5 μM) was incubated with 4 M guanidine hydrochloride in 10 mM HEPES, pH 7, causing the release of bound Zn^{2+} as the enzyme unfolds. To this solution was added 0.1 mM PAR; chelation of Zn^{2+} by PAR causes an increase in the absorption of PAR at 500 nm. The absorbance change can be related to the original concentration of bound Zn^{2+} in LpxC by comparison with a Zn^{2+} standard curve (0−6 μM $ZnSO_4$). Varied concentrations of metal-free LpxC (2−5 μM) were included in the Zn^{2+} standard solutions used for the standard curves in order to account for effects of the LpxC protein on the PAR response.

Preparation of Metal-Free Deacetylase. To prepare metal-free *E. coli* LpxC, purified deacetylase (1−25 mL of ~150 μM) was incubated with 20 mM DPA in 10 mM HEPES, pH 7, for 10−30 min on ice. The reaction was then diluted 2−3-fold into 25 mM HEPES, pH 7, and concentrated 5−10-fold in an Amicon ultrafiltration device with a YM-10 membrane. The dilution/concentration procedure was repeated until the concentration of DPA in the sample was estimated to be less than 1 mM. The sample was then concentrated to a volume of less than 5 mL, and the remaining DPA was removed on a PD-10 gel filtration column (Pharmacia) equilibrated in 25 mM HEPES, pH 7. The concentration of residual Zn^{2+} in the enzyme preparation was determined to be < 0.1 mol/mol of enzyme by the ICP and PAR assays. Apo-LpxC stocks were stored at high

concentrations (>100 μM) in plastic microcentrifuge tubes at −80 °C to prevent significant levels of recontamination by Zn^{2+}. The apo-deacetylase is stable for at least 6 months stored under these conditions. However, the enzyme may become contaminated with Zn^{2+} leaching out of the plastic after longer storage times as evidenced by increased activity of older apoenzyme preparations in the absence of added Zn^{2+}.

Preparation of Zn^{2+}-Reconstituted Deacetylase. Metal-free LpxC (prepared as described above) was reconstituted with Zn^{2+} under two different conditions. To prepare LpxC containing a single Zn^{2+} per protein molecule, apo-LpxC (1 L of 2.5 μM) was incubated with 2.5 μM $ZnSO_4$ for 30 min on ice. This solution was then concentrated 50−100-fold, and any remaining unbound Zn^{2+} was removed on a 60 mL Bio-Gel P6 (BioRad) gel filtration column. The Zn^{2+} content of the resultant protein was determined to be 0.95 Zn^{2+}/LpxC using the colorimetric PAR assay. A second preparation of Zn^{2+}-LpxC was made by incubating apo-LpxC (10 mL of 200−300 μM) with a 2-fold excess concentration of $ZnSO_4$ for 30 min on ice. Any remaining unbound Zn^{2+} was removed by gel filtration (Bio-Gel P6, 60 mL), and the Zn^{2+} concentration of this LpxC was determined to be 2 Zn^{2+}/LpxC using both PAR and ICP analysis.

Preparation of Substrates. [α-^{32}P]-labeled UDP-*N*-acetylglucosamine (UDP-GlcNAc) was prepared using the method described by Kelly and colleagues (*21*). UDP-GlcNAc either was used directly as a slowly reacting substrate or was further acylated to generate the physiological deacetylase substrate, UDP-3-*O*-(*R*-3-hydroxymyristoyl)GlcNAc (UDP-3-*O*-acyl-GlcNAc). The acylation reaction was catalyzed by *E. coli* LpxA protein (*7*) (generously provided by T. J. O. Wyckoff, Duke University), and UDP-3-*O*-acyl-GlcNAc was purified as described (*21*) except that 1 mM methylmethanethiosulfonate was included in the acylation reaction catalyzed by LpxA which increased the product yield 2-fold. This is presumably due to alkylation of the free thiol of ACP, a product of the thermodynamically unfavorable acylation reaction (*7*). Also, a high concentration of LpxA (0.05 mg/mL) was used to shorten the reaction time, decreasing the amount of UDP-3-*O*-acyl-GlcNAc that rearranges to the inactive 4- or 6-acyl isomer (*5*).

Deacetylase Assay. Initial rates of LpxC-catalyzed deacetylation of the physiological substrate, UDP-3-*O*-acyl-GlcNAc, were determined at 30 °C or 1 °C in 40 mM bis-tris, pH 5.5−6.0, as specified for each assay, in a final reaction volume of 20−30 μL. Reactions were initiated by dilution of enzyme into a reaction mixture containing buffer and [α-^{32}P]-labeled substrate (0.5−30 μM, 1×10^6−10^7 cpm/nmol), such that the final concentration of LpxC in the assay was 1−5 nM (30 °C assay) or 0.1−1 μM (1 °C assay). Bovine serum albumin (1 mg/mL) was also included in assays with low enzyme concentrations (<1 μM). A portion of each reaction (5 μL) was removed at various times, selected so that the total conversion to product was less than 10%, and the reaction was stopped by mixing with 1 μL of 1.25 M NaOH and incubated at 30 °C for 10 min. The base catalyzes the cleavage of the ester-linked *R*-3-hydroxymyristoyl chain from the substrate and the product, yielding UDP-GlcNAc and UDP-glucosamine, respectively. The reactions were neutralized by the addition of 1 μL of 1.25 M acetic acid and 1 μL of 5% trichloroacetic acid, incubated on ice for 5 min, and then clarified by centrifugation. A 2 μL portion of each sample was spotted on a PEI−cellulose TLC plate and developed in a 0.2 M guanidine hydrochloride solvent system to resolve the product from substrate, as previously described (*22*). The radioactivity on the plates was analyzed using a PhosphorImager and ImageQuant software (Molecular Dynamics, Inc.) to quantify the amount of product.

Activity assays using UDP-GlcNAc as the substrate were performed at 30 °C in the same way as for the physiological substrate, except that the concentrations of enzyme and substrate were increased to 10−50 μM LpxC and 0.25−10 mM [α-^{32}P]-UDP-GlcNAc (1×10^3−10^4 cpm/nmol). The reactions containing UDP-GlcNAc were still stopped by the addition of 1.25 M NaOH; however, the additional 10 min incubation at 30 °C before neutralization with acid was not necessary.

Steady-state kinetic parameters and standard errors for deacetylation of UDP-3-*O*-acyl-GlcNAc were determined by a fit of the initial velocities to the Michaelis−Menten equation (*23*), using the Kaleidagraph (Synergy Software) curve-fitting program. The steady-state k_{cat}/K_M for UDP-GlcNAc was measured from the linear portion (0.25−10 mM) of the velocity vs substrate plot using Kaleidagraph, and a corresponding lower limit to k_{cat} and K_M for UDP-GlcNAc was estimated from these data.

Inhibition by EDTA and DPA. LpxC (0.25 μM) was added to a solution containing 5 μM EDTA in 40 mM bis-tris, pH 6.0, 1 mg/mL BSA, and incubated at 1 °C. At various times after the addition of LpxC, an 8 μL portion was removed to an assay tube (final volume = 20 μL) containing 4 μM UDP-3-*O*-acyl-GlcNAc in the same buffer. Additional EDTA was added to the reaction mixture to maintain 5 μM EDTA in the assay. Initial velocities of each reaction were determined and fit to a single exponential decrease in activity as a function of time of incubation with 5 μM EDTA. The concentration dependence for EDTA inhibition of LpxC was also measured by incubating LpxC (0.25 μM) with 0.5−10 μM EDTA for 30−45 min at 1 °C in 40 mM bis-tris, pH 6.0, containing 1 mg/mL BSA. The LpxC/EDTA stocks were then diluted 2.5-fold into an assay mix containing 4 μM UDP-3-*O*-acyl-GlcNAc, and the initial velocity of product formation was measured. Assays were supplemented with EDTA to maintain the same concentration of chelator as in the preincubation. The concentration dependence for DPA inhibition of LpxC was measured in the same way, except with a shorter (15−20 min) preincubation with DPA (1−100 μM) since inhibition by DPA is complete within the time required to initiate the assays.

Inhibition by Zn^{2+}. LpxC (2.5 nM in 40 mM bis-tris, pH 5.5, 30 °C, or 0.25 μM in 40 mM bis-tris, pH 6.0, 1 °C) was incubated with varied concentrations of $ZnSO_4$ for 10−30 min on ice, in the presence of 1 mg/mL BSA. The enzyme/Zn^{2+} stock was then diluted 2.5-fold into an assay mix containing 4 μM UDP-3-*O*-acyl-GlcNAc at the indicated temperature and buffer conditions. Initial velocities at each concentration of $ZnSO_4$ were determined; the data were expressed as a percentage of the activity in the absence of added Zn^{2+} and fit to eq 1, as a function of total Zn^{2+} concentration in the preincubation, to yield the IC_{50} for Zn^{2+} at each temperature:

$$v_i/v_c = IC_{50}/([ZnSO_4] + IC_{50}) \quad (1)$$

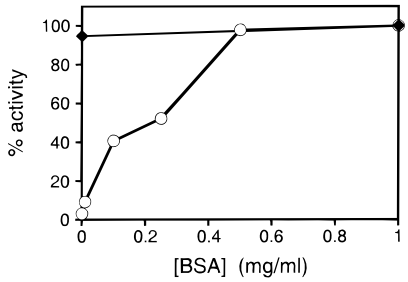

FIGURE 2: BSA stabilization of LpxC activity. LpxC (2.5 nM) was incubated with increasing concentrations of BSA and then diluted 2.5-fold into the reactions to yield final concentrations of 1 nM LpxC and 0.001−1 mg/mL BSA. Reactions were performed at 30 °C in 40 mM bis-tris, pH 5.5, with 4 μM UDP-3-*O*-acyl-GlcNAc (○). In a second experiment, 25 μM LpxC was also incubated with or without BSA and diluted into an assay (final [LpxC] = 10 μM, final [BSA] = 0 or 1 mg/mL) containing 1 mM UDP-GlcNAc in 40 mM bis-tris, pH 5.7 at 30 °C (◆). Activities are reported as a percentage of the maximal activity (at 1 mg/mL BSA) observed in each experiment.

RESULTS

To investigate the catalytic mechanism of *E. coli* LpxC, we have determined the metal ion requirement of this enzyme. Using plasma emission spectroscopy and colorimetric methods, we demonstrated that the LpxC protein purified from *E. coli* contains a significant amount of bound zinc ions that cannot be removed by gel filtration. To determine whether this bound Zn^{2+} is essential for catalytic activity, we first developed conditions to assay the deacetylase activity of the purified protein. Using these conditions, we then investigated the dependence of the activity of LpxC on the concentration of Zn^{2+} and other divalent cations.

BSA Requirement for Optimal LpxC Activity. To obtain high deacetylase activity, the standard 30 °C assay conditions (*6*) require the addition of 1 mg/mL BSA. Deacetylase activity in the absence of BSA is undetectable under these conditions when the concentration of LpxC in the assay is 1−5 nM. However, BSA alone does not catalyze deacetylation of the LpxC substrate. At low concentrations of LpxC (1−5 nM), the loss of activity is dependent on the concentration of BSA in the assay with ≥0.5 mg/mL BSA required for maximal activity (Figure 2). This activity loss is time-dependent, with a $t_{1/2}$ of 3 min after dilution into 40 mM bis-tris, pH 5.5, buffer containing no BSA (final [LpxC] = 1 nM). The loss of activity is also reversible. Incubation of 10 nM LpxC in buffer without BSA for 30 min completely inactivates the enzyme; however, when this enzyme is diluted further (4-fold) into buffer containing 1 mg/mL BSA, 100% of the activity is restored when assayed after a 2 h incubation (data not shown). A number of other components were tested for their ability to replace BSA in the assay to prevent loss of LpxC activity under the 30 °C reaction conditions, including the following: 1 or 10 μM Zn^{2+}, 1 μM Fe^{2+}, 10% glycerol, 0.5 or 3% poly(ethylene glycol), 0.1 or 1% Triton X-100, 0.1 or 1 μM DTT or tris(2-carboxyethyl)phosphine (TCEP), 1 mg/mL IgG, 1 or 10 μM EDTA, 1 mM palmitate or myristate, and 40 mM HEPES, pH 8.0. However, none of these reagents were able to substitute for BSA (data not shown). Furthermore, pretreatment of the BSA by overnight dialysis against the metal-chelating reagent Chelex-100 did not diminish the activation of LpxC by BSA.

Other cases of enzymes that depend on the presence of BSA for maintaining optimal activity are known, including isocitrate dehydrogenase and HIV-1 protease (*24*, *25*). In these cases, the BSA requirement can be diminished or eliminated at high enzyme concentrations. Therefore, to slow the reaction rate enough to increase the concentration of LpxC in the assay to 1 μM, we decreased the temperature of the reaction to 1 °C. With 1 μM LpxC assayed at 1 °C, the observed activation by the addition of 1 mg/mL BSA is small (<2-fold), and the enzyme maintains a high level of activity for at least 1 h in the absence of BSA (data not shown). Activity assays using a poor deacetylase substrate, UDP-GlcNAc, can be performed with even higher LpxC concentrations, ≥10 μM, where 1 mg/mL BSA has no effect on the deacetylase activity (Figure 2).

Some suggested roles for BSA activation of other enzymes include stabilization of protein structure or oligomers, reduction of important sulfhydryl groups, and/or chelation of inhibitory metal ions or provision of stimulatory metal ions since BSA has several metal binding sites (*26*). The dependence of activity on the concentration of LpxC suggests that there may be a catalytically important oligomerization of LpxC and that BSA may stabilize the oligomeric form at low enzyme concentrations. However, no indication of any higher order molecular states is seen with analytical ultracentrifugation experiments on the purified LpxC protein (data not shown). Additionally, the inability of DTT, TCEP, or EDTA to replace BSA at low LpxC concentrations (1−5 nM) suggests that BSA is not functioning solely as a reductant or metal ion chelator. However, the extent of activity loss in the absence of BSA can be diminished at higher LpxC concentrations (0.1−1 μM) by treating the substrate and buffers with Chelex-100 and by removing excess Zn^{2+} in the enzyme preparation, suggesting that one of the functions of BSA is to chelate inhibitory metal ions. Since 1−10 μM Zn^{2+} also cannot substitute for BSA, BSA is not enhancing activity by increasing the Zn^{2+} concentration in the assay and reconstituting the active site metal ion. Moreover, no evidence for additional stimulatory metal ions has been seen in reconstitution experiments at high concentrations of apo-LpxC, all of which have been performed in the absence of BSA. Therefore, it is unlikely that BSA is stimulating activity under these conditions by providing Zn^{2+} or other stimulatory metals. Although the effect of BSA on activity is not yet completely understood, high concentrations of LpxC in the assays can eliminate the BSA requirement, allowing for the measurement of stimulation by metal ions without the complications of metal ion buffering and contamination by BSA (Figure 2).

LpxC Contains Bound Zn^{2+}. Inductively coupled plasma emission spectroscopy (ICP) and a Zn^{2+} colorimetric assay indicated that purified LpxC contains multiple bound zinc ions. The actual concentration of bound Zn^{2+} varied with different enzyme preparations from a low of 1.3 mol of Zn^{2+}/mol of LpxC to a high of 3.2 mol of Zn^{2+}/mol of LpxC, with an average Zn^{2+} content of ≈2 mol of Zn^{2+}/mol of LpxC. No other bound metal ions (<0.1 mol/mol of LpxC) were detected in purified LpxC by the 23 element ICP analysis. The bound Zn^{2+} could be readily removed from LpxC by incubation with DPA, and the bound zinc ions could be easily reconstituted by incubation with Zn^{2+} (Table 1). To compensate for the differences in Zn^{2+} content between

Table 1: Metal Analysis of LpxC Protein

	PAR colorimetric assay (Zn^{2+}/protein)	ICP (Zn^{2+}/protein)
apo-LpxC[a]	<0.1	0.06
1:1 reconstituted LpxC[b]	0.95 ± 0.3	ND[c]
2:1 reconstituted LpxC[b]	2.2 ± 0.2	2.0 ± 0.06

[a] Apo-LpxC was prepared by incubation with 20 mM DPA as described under Materials and Methods. ICP samples contained 50 μM Zn^{2+}-reconstituted LpxC or 97 μM apo-LpxC, and PAR samples contained 2−5 μM Zn^{2+}-reconstituted LpxC or 5−10 μM apo-LpxC. [b] 1:1 and 2:1 Zn^{2+}-reconstituted deacetylase was prepared from apo-LpxC as described under Materials and Methods. Free zinc was removed by gel filtration before metal analysis of each sample. [c] ND = not determined.

different enzyme preparations, we set out to prepare Zn^{2+}-LpxC with a defined stoichiometry for functional studies. Apo-LpxC was incubated with a known concentration of Zn^{2+} in either a 1:1 or a 2:1 Zn^{2+}:LpxC stoichiometry (Table 1). When assayed at 1 °C in the absence of 1 mg/mL BSA, the activity of 2:1 reconstituted LpxC was ∼35% lower than that of the 1:1 Zn^{2+}: LpxC preparation, likely due to binding of inhibitory Zn^{2+} as described below. However, when BSA was included in the enzyme assay, the activity of the two enzymes was identical within experimental error, suggesting that under these conditions BSA functions as a chelator of inhibitory metal ions. All of the steady-state kinetic analyses and inhibition studies with the physiological LpxC substrate, UDP-3-*O*-acyl-GlcNAc, were performed with the 2:1 reconstituted LpxC in the presence of 1 mg/mL BSA to relieve inhibition by the second zinc ion.

Steady-State Kinetic Parameters. To characterize the steady-state activity of this enzyme, we measured the dependence of LpxC activity on the concentration of the physiological deacetylase substrate, UDP-3-*O*-acyl-GlcNAc, at 30 and 1 °C in assays containing 1 mg/mL BSA. The data are well described by the Michaelis−Menten equation, and the calculated steady-state kinetic parameters are listed in Table 2. Decreasing the temperature to 1 °C decreases the value for k_{cat} almost 40-fold, while k_{cat}/K_M and K_M are decreased 10-fold and 3.5-fold, respectively.

Additionally, we demonstrated that LpxC also catalyzes deacetylation of UDP-GlcNAc. We measured the steady-state k_{cat}/K_M for this alternative deacetylase substrate at 30 °C in the absence of BSA (Table 2), since at high enzyme concentrations (>10 μM) BSA does not increase catalytic activity. For these experiments, we used the 1:1 Zn^{2+}:LpxC preparation that does not contain a second, inhibitory Zn^{2+}. The k_{cat}/K_M for UDP-GlcNAc is (5×10^6)-fold lower than the k_{cat}/K_M for the physiological substrate, UDP-3-*O*-acyl-GlcNAc, demonstrating that the ester-linked acyl chain is essential for efficient catalysis (Table 2). Since LpxC activity is linearly dependent ($R = 0.999$) on the concentration of UDP-GlcNAc up to 10 mM, a lower limit for the steady-state K_M and k_{cat} is 20 mM and 0.006 s^{-1}, respectively.

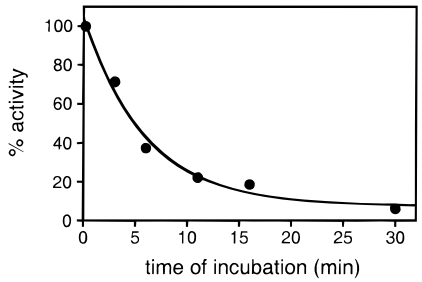

FIGURE 3: Time dependence of EDTA inhibition. LpxC activity (0.1 μM enzyme) was measured at 4 μM UDP-3-*O*-acyl-GlcNAc, 1 °C, in 40 mM bis-tris, pH 6.0, in the presence of 1 mg/mL BSA, after incubation with 5 μM EDTA for various times (0−30 min). Activity is expressed as the percentage of activity remaining after incubation for the indicated amount of time. The data were fit to a single-exponential decrease as a function of time of incubation, yielding $t_{1/2} = 4 \pm 1$ min.

Inhibition by Metal-Directed Chelators. To investigate whether the Zn^{2+} bound to the purified deacetylase is important for catalytic activity, we determined whether metal chelators, such as EDTA and DPA, inhibit LpxC. EDTA completely inhibits the deacetylase (<1% remaining activity) in a time-dependent manner that can be described as an exponential decrease with a $t_{1/2}$ of 4 ± 1 min at 5 μM EDTA at 1 °C (Figure 3). Time-dependent inhibition of LpxC activity by EDTA under the 30 °C assay conditions was also observed; however, higher concentrations of EDTA (>10 μM) were required. In contrast, inhibition of LpxC by DPA is very fast; inhibition by 20 μM and 100 μM DPA is complete within the time required to add inhibitor and start the assay (<10 s) (data not shown). The concentration dependence of inhibition of LpxC by EDTA was investigated at pH 6, 1 °C in the presence of 1 mg/mL BSA (Figure 4). Inhibition by EDTA is nearly complete at low concentrations of chelator; half of the enzyme activity is lost at ≈1 μM EDTA under these conditions. DPA also completely inhibits LpxC activity, and the concentration dependence of DPA inhibition at pH 6, 1 °C in the presence of 1 mg/mL BSA is shown in Figure 4, yielding an IC_{50} for inhibition of ≈25 μM. Additionally, we have demonstrated that incubation of LpxC with DPA leads to the removal of the bound zinc ion (Table 1). The complete activity loss in the presence of both

Table 2: Steady-State Kinetic Parameters for LpxC Activity[a]

substrate	conditions	k_{cat} (s^{-1})	K_M (μM)	k_{cat}/K_M (M^{-1} s^{-1})
UDP-3-*O*-acyl-GlcNAc	pH 5.7 1 °C	0.09 ± 0.01	0.6 ± 0.3	(0.14 ± 0.03) × 10^6
UDP-3-*O*-acyl-GlcNAc	pH 5.5 30 °C	3.3 ± 0.2	2.1 ± 0.5	(1.5 ± 0.1) × 10^6
UDP-GlcNAc	pH 5.7 30 °C	>0.006[b]	>20000[b]	0.28 ± 0.06

[a] Initial rates of deacetylation were determined under the conditions indicated for each substrate using the standard LpxC assay described under Materials and Methods. Activity with UDP-3-*O*-acyl-GlcNAc was determined in the presence of 1 mg/mL BSA using 0.5−10 μM substrate and 0.1 μM enzyme (1 °C) or 0.5−25 μM substrate and 1−5 nM enzyme (30 °C). Activity with UDP-GlcNAc was determined in the absence of BSA using 0.25−10 mM substrate and 50 μM enzyme. [b] No curvature was observed in a plot of rate versus [UDP-GlcNAc] up to 10 mM, allowing for estimation of only a lower limit for the value of k_{cat} and K_M.

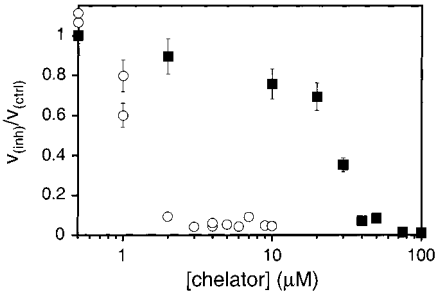

FIGURE 4: Concentration dependence of inhibition by chelators. Activity of *E. coli* LpxC (0.1 μM) with 4 μM UDP-3-*O*-acyl-GlcNAc was determined at 1 °C in 40 mM bis-tris, pH 6.0, in the presence of 1 mg/mL BSA and various concentrations of EDTA and DPA. LpxC (0.25 μM) was incubated with EDTA (○) (0.5−10 μM, 30−45 min) or DPA (■) (1−100 μM, 15−20 min) on ice, prior to dilution of the enzyme 2.5-fold into an assay containing the same concentration of EDTA or DPA as in the preincubation. LpxC activity is decreased to <10% of the original activity in the presence of high concentrations of either chelator, and the activity is decreased 50% at ≈1 μM EDTA or ≈25 μM DPA.

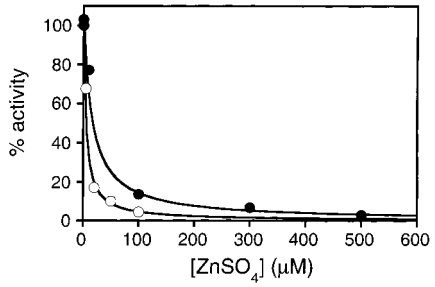

FIGURE 5: Zn^{2+} inhibition of LpxC activity. LpxC was incubated for 10−30 min with Zn^{2+} (0−500 μM total Zn^{2+}) and 1 mg/mL BSA in 40 mM bis-tris, pH 5.5, 30 °C, or 40 mM bis-tris, pH 6, 1 °C. The assay was initiated by dilution of the enzyme 2.5-fold into the assay containing the same buffer conditions, and activity was measured using 4 μM UDP-3-*O*-acyl-GlcNAc and 1 nM LpxC at 30 °C (●) or 0.1 μM LpxC at 1 °C (○). LpxC activity is expressed as a percentage of the velocity in the absence of added Zn^{2+} and plotted against the total concentration of $ZnSO_4$ in the preincubation with LpxC. The data were fit to eq 1 for determination of the IC_{50} for inhibition under these conditions; the IC_{50} values were 24 ± 4 μM at 30 °C and 7 ± 2 μM at 1 °C.

of these metal ion chelators suggests that a metal ion, presumably Zn^{2+}, bound to LpxC is essential for catalysis.

Inhibition by Zn^{2+}. As observed with several other Zn^{2+} metalloenzymes (*27*, *28*), LpxC is also inhibited by micromolar concentrations of total zinc ions (Figure 5). The IC_{50} for Zn^{2+} inhibition of LpxC activity was 7 ± 2 μM in 40 mM bis-tris, pH 6 at 1 °C, and 24 ± 4 μM in 40 mM bis-tris, pH 5.5 at 30 °C. This inhibition is likely due to zinc ions binding to additional metal binding sites in the protein since we have measured a stoichiometry of ≥2 Zn^{2+}/LpxC after incubation with high (400−600 μM) concentrations of Zn^{2+} (Table 1).

Zinc Requirement for Deacetylase Activity. To investigate the role of the bound Zn^{2+} in more detail, we directly measured the dependence of LpxC activity on the presence of Zn^{2+}. The Zn^{2+} in LpxC was easily removed by incubation with 20 mM DPA followed by gel filtration chromatography (Table 1). The activity of apo-LpxC was assayed using the less active UDP-GlcNAc substrate so that in the assay the LpxC concentration could be increased to 50 μM and BSA could be eliminated, thus limiting problems with environmental metal ion contamination. The deacetylase activity of

Table 3: Effects of Metal Substitution on LpxC Activity

metal ion	v_o (μM/h)[a]	$[Me^{2+}]/[LpxC]$[b]	relative activity[c]
apo (none)	9	−	0.11
Zn^{2+}	81	0.6	1
Cd^{2+}	7	1	0.09
Ca^{2+}	9	1	0.11
Cu^{2+}	3	1	0.04
Mg^{2+}	10	1	0.12
Mn^{2+}	31	1	0.38
Ni^{2+}	230	3[d]	2.9
Co^{2+}	250	1	3.1

[a] Initial rates of LpxC activity after incubation of apo-LpxC with the indicated metal ions were determined using 50 μM enzyme and 1 mM UDP-GlcNAc in 40 mM bis-tris, pH 5.7, at 30 °C. [b] The velocities indicated in the previous column were determined at the indicated Me^{2+}:LpxC ratio such that the maximal levels of activity with each different metal were observed. [c] The activity relative to the maximal Zn^{2+}-LpxC activity. [d] The higher stoichiometry for Ni^{2+} is due to the decreased metal affinity (see Figure 7A).

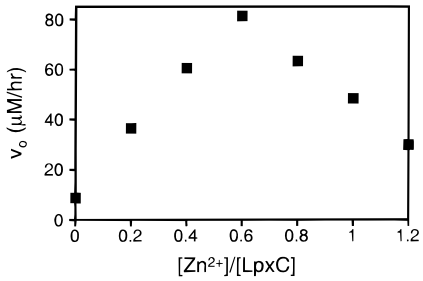

FIGURE 6: Stimulation of apo-LpxC activity by addition of Zn^{2+}. Apo-LpxC (125 μM) was incubated with increasing concentrations of $ZnSO_4$ (0−150 μM) in 40 mM bis-tris, pH 5.7, for 40 min on ice and then diluted 2.5-fold into an activity assay containing 1 mM UDP-GlcNAc in 40 mM bis-tris, pH 5.7 at 30 °C. Activity increased until a Zn^{2+}:LpxC ratio of 0.6:1 was attained, and then activity decreased due to inhibition by Zn^{2+}.

50 μM apo-LpxC with 1 mM UDP-GlcNAc was 9 μM/h (Table 3), due to the small concentration of residual Zn^{2+}-LpxC in the apo-LpxC preparation (see Table 1). Increasing concentrations of total Zn^{2+} (up to 150 μM) were incubated with apo-LpxC (125 μM) which was then diluted 2.5-fold into the assay. As Zn^{2+} ions were added to apo-LpxC, activity increased linearly until the Zn^{2+}:LpxC ratio was 0.6:1 (Figure 6). However, the activity decreased upon further Zn^{2+} addition. This decrease in activity is likely caused by Zn^{2+} binding to inhibitory sites on LpxC (see Figure 5). Therefore, the maximal rate of deacetylation observed when assayed at 50 μM enzyme and 1 mM UDP-GlcNAc (81 μM/h) is likely less than the true maximal activity, due to inhibition by Zn^{2+}. In fact, extrapolation of the initial portion of the activity vs $[Zn^{2+}]$ plot to a ratio of 1:1 Zn^{2+}:LpxC suggests that the true maximal activity is ≈130 μM/h. In this case, the background activity of apo-LpxC in the absence of Zn^{2+} would be 7% of the maximal Zn^{2+}-LpxC activity, consistent with the 6−10% level of Zn^{2+}-LpxC that remains in the apo-LpxC preparation (see Table 1). These data demonstrate that Zn^{2+} is required for optimal deacetylase activity. However, to determine the optimal metal:LpxC stoichiometry, we examined the reconstitution of LpxC activity with other metal ions.

Reconstitution of Deacetylase with Other Metals. To investigate further the role of the metal ion in LpxC, we determined which metal ions could substitute for the native Zn^{2+} in LpxC. Again, to minimize background metal

contamination, reconstituted enzyme was assayed at high LpxC concentrations (50 μM) with the UDP-GlcNAc substrate in the absence of BSA. Divalent metal ions were incubated with apo-LpxC (125 μM Me^{2+} incubated with 125 μM apo-LpxC), and diluted 2.5-fold into the assay containing 1 mM UDP-GlcNAc at 30 °C in 40 mM bis-tris, pH 5.7. The activity of LpxC in the presence of Cd^{2+}, Ca^{2+}, Cu^{2+}, and Mg^{2+} is equal to or below the activity of apo-LpxC (Table 3), indicating that these metal ions are ineffective at substituting for Zn^{2+} at these stoichiometric concentrations. Furthermore, higher concentrations of Cu^{2+}, Ca^{2+}, and Mg^{2+} (375 μM Me^{2+} incubated with 125 μM apo-LpxC) did not activate apo-LpxC. Additionally, we demonstrated that Cu^{2+} binds to LpxC. After removal of free Cu^{2+} from the 125 μM apo-LpxC/Cu^{2+} enzyme stock by gel filtration chromatography, ≈1 mol of Cu^{2+}/mol of LpxC was observed, as assayed using the PAR assay with a 0−6 μM $CuSO_4$ standard curve (data not shown). This indicates that, at least for Cu^{2+}, the low activity observed in the assay was not due to inefficient metal binding to the enzyme.

Incubation of apo-LpxC (125 μM) with stoichiometric amounts of Mn^{2+}, Co^{2+}, and Ni^{2+} reactivates apo-LpxC to varying degrees ($Co^{2+} \approx Ni^{2+} > Zn^{2+} > Mn^{2+}$) (Table 3). Higher concentrations of Mn^{2+} or Co^{2+} (up to 375 μM) did not further stimulate LpxC activity. However, when the concentration of Ni^{2+} in the incubation with apo-LpxC was increased to 375 μM (3:1 Ni^{2+}:LpxC), the activity was enhanced (see Figure 7A).

A similar pattern of metal reconstitution of LpxC was observed with the physiological substrate in that Zn^{2+}, Co^{2+}, and Ni^{2+} were all able to stimulate apo-LpxC activity (data not shown). However, since assays with the physiological substrate must be performed at lower enzyme concentrations (1 μM LpxC), they were complicated by a 20−30% background level of apo-LpxC activity due to contaminating Zn^{2+} in the assays. Attempts were made to decrease the contaminating Zn^{2+} by treatment of all buffers and substrate with Chelex-100 (BioRad) or Chelating Sepharose (Pharmacia) resins, use of plastic microcentrifuge tubes washed with 5 μM EDTA, and use of high-quality plastic pipet tips. While these precautions were successful at preventing Zn^{2+} contamination in control experiments with another Zn^{2+}-metalloenzyme, carbonic anhydrase II, they were not sufficient for preventing high background activities with apo-LpxC in the absence of added metal ions.

The concentration dependence of reactivation by Ni^{2+} and Co^{2+} was investigated. When deacetylase activity is measured as a function of the total concentration of Ni^{2+}, the activity increase at low concentration is not linear and the activity continues to increase up to 375 μM Ni^{2+} (3:1 Ni^{2+}:LpxC), suggesting that Ni^{2+} does not bind stoichiometrically to the enzyme under these conditions (Figure 7A). A fit of these data to a binding isotherm suggests that the apparent K_D for Ni^{2+} is 37 ± 4 μM, indicating that the affinity of the enzyme for Ni^{2+} is decreased significantly compared to Zn^{2+}. On the other hand, apo-LpxC activity increases linearly with [Co^{2+}] until a stoichiometry of 1:1 Co^{2+}:LpxC is achieved, and the activity remains at this level even at higher (up to 375 μM) Co^{2+} concentrations (Figure 7B). Unlike Zn^{2+}, Co^{2+} is not inhibitory in this concentration range since the titration of apo-LpxC with Co^{2+} does not show a decrease in activity at high metal ion concentrations. This result indicates that

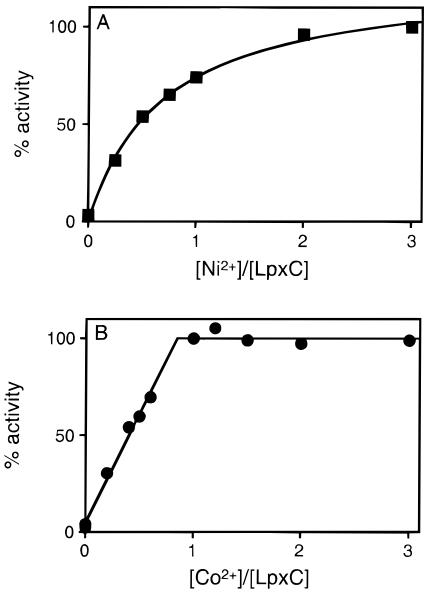

FIGURE 7: (A) Stimulation of LpxC activity by Ni^{2+}. Apo-LpxC (125 μM) was incubated for 10 min at room temperature with increasing concentrations of total $NiSO_4$ (0−375 μM), and then used to initiate the reaction by a 2.5-fold dilution into the assay containing 1 mM UDP-GlcNAc in 40 mM bis-tris, pH 5.7, at 30 °C. Activities are expressed as a percentage of the highest activity observed with Ni^{2+}. The data were fit to a binding isotherm against the concentration of Ni^{2+} in the assay, yielding an apparent K_D for Ni^{2+} of 37 ± 4 μM. (B) Stimulation of LpxC activity by Co^{2+}. Initial rates of LpxC-catalyzed deacetylation of UDP-GlcNAc (1 mM) were determined in 40 mM bis-tris, pH 5.7, at 30 °C. Apo-LpxC (125 μM) was incubated with increasing concentrations of $CoSO_4$ (0−375 μM) for 10 min at room temperature prior to the start of the reaction. The enzyme stock was diluted 2.5-fold into the assay to start the reaction, resulting in a final enzyme concentration of 50 μM. Activities are expressed as a percentage of the maximal activity observed with Co^{2+} at a stoichiometry of 1 mol of Co^{2+}/mol of LpxC.

the Co^{2+}:LpxC stoichiometry required for maximal activity is 1:1. The high activity of Co^{2+}-LpxC (Table 3) indicates that Co^{2+} is a good replacement for the Zn^{2+} in LpxC, as it is in several other zinc metalloenzymes (*29*−*31*), and therefore the stoichiometry of the maximally active Zn^{2+}-LpxC is likely the same.

DISCUSSION

We have demonstrated that *E. coli* LpxC, which catalyzes the committed step in the production of lipid A, contains bound Zn^{2+} that is required for optimal enzyme activity. LpxC activity is inhibited by incubation with several metal ion chelators, including EDTA and DPA, as well as high concentrations of Zn^{2+}. Inhibition by such reagents suggests, but is not proof, that LpxC is a metalloenzyme. Therefore, we directly demonstrated that removal of the Zn^{2+} ion from *E. coli* LpxC causes a significant loss of the deacetylase activity that can be restored by addition of Zn^{2+}. We also showed that the stoichiometry of the active metal/LpxC complex is 1:1 using Co^{2+}, a noninhibitory metal ion. These data suggest that LpxC with a single properly bound Zn^{2+} is the active form.

Deacetylase Substrate Specificity. LpxC catalyzes deacetylation of the physiological substrate, UDP-3-*O*-acyl-GlcNAc, with a k_{cat}/K_M at 30 °C of 1.5×10^6 M^{-1} s^{-1}, well below the diffusion controlled limit of $\sim 10^8$ M^{-1} s^{-1} (*23*). This suggests

that some step other than substrate association is rate-limiting under these conditions. The 10-fold decrease in k_{cat}/K_M that is observed at 1 °C is entirely due to a decrease in the steady-state k_{cat} at the lower temperature, since K_M is actually somewhat lower under these conditions.

In *E. coli*, UDP-3-*O*-acyl-GlcNAc is the only physiological LpxC substrate identified to date. The determinants of substrate specificity can be investigated by removing or altering functional groups in the substrate. Additionally, less efficient substrates can be very beneficial in the study of metalloenzymes, allowing the use of high enzyme concentrations to decrease the effect of any background metal contamination in the assays. Previously, using crude *E. coli* cell extracts as the source of LpxC, substitution of propyl, butyl, pentyl, and hexyl moieties for the native acetyl group at the 2-N position of the LpxC substrate has been demonstrated to decrease the relative rate of reactivity as a function of increasing chain length, from 90% of the UDP-3-*O*-acyl-GlcNAc activity with a propyl substitution to <0.1% with the hexyl substitution (*32*). This suggests that the binding site for the LpxC substrate may be constrained such that larger groups at the 2-N position are not easily accommodated.

In this work, we demonstrated that LpxC catalyzes deacetylation of UDP-GlcNAc, a substrate analogue with the ester-linked acyl chain removed, but the value of k_{cat}/K_M is decreased (5×10^6)-fold compared to UDP-3-*O*-acyl-GlcNAc. This decreased efficiency is at least partially due to a $\geq 10^4$-fold increase in K_M (Table 2). The impaired activity of UDP-GlcNAc indicates the importance of the hydrophobic character of this acyl chain for optimal binding and reactivity and may also have implications for the design of specific deacetylase inhibitors for use as antibacterial agents. Consistent with this hypothesis, in the series of hydroxamate compounds investigated by Onishi and colleagues (*4*), the K_i decreased upon the addition of hydrophobic groups to the phenyl ring on the original lead compound. Taken together, these data suggest that the LpxC active site is specific for several features of the physiological LpxC substrate, and these characteristics must be taken into account in the design of LpxC inhibitors.

Time Dependence of Inhibition by Chelators. Inhibition of Zn^{2+} metalloenzymes by chelators can occur by removing the bound Zn^{2+} from the enzyme or by forming a stable enzyme−Zn^{2+}−inhibitor ternary complex. The fast inhibition by DPA suggests that this chelator catalyzes the removal of Zn^{2+} from LpxC by forming a ternary enzyme−Zn^{2+}−DPA complex that is either inactive itself or decays quickly to inactive apoenzyme and Zn^{2+}−DPA. Removal of Zn^{2+} from the enzyme by DPA is corroborated by the fact that metal-free apoenzyme is rapidly prepared by incubation with DPA. Small-molecule chelators inhibit a number of other Zn^{2+} metalloenzymes, including carboxypeptidase A, by removal of the zinc ion (*33*, *34*).

In contrast with DPA, the time dependence of EDTA inhibition (Figure 3) is consistent with a mechanism in which EDTA chelates Zn^{2+} as it spontaneously dissociates from the enzyme or in which there is a slow dissociation of an enzyme−Zn^{2+}−EDTA complex to inactive apo-LpxC and EDTA−Zn^{2+}. A similar difference in the time dependence of metal removal by different chelators has been observed with the enzyme carbonic anhydrase; this metalloenzyme also exhibits slow Zn^{2+} dissociation in the presence of EDTA and catalysis of Zn^{2+} dissociation by DPA (*35*).

In previous reports, deacetylase activity in crude extracts of *E. coli* bearing the wild-type LpxC protein was not inhibited by the presence of even 0.5 mM EDTA (*12*), a concentration that is well above the IC_{50} for EDTA inhibition measured in this work. However, the high concentrations of cations in the *E. coli* crude extract likely reduce the effectiveness of the EDTA chelator. Inactivation of *E. coli* LpxC activity by EDTA was observed with extracts of cells that contained a mutation (envA1) in LpxC (*12*) which may decrease the affinity of LpxC for Zn^{2+} and thereby increase the sensitivity of this enzyme to EDTA. Time-dependent inactivation by EDTA has also been observed with both crude extracts and purified LpxC from *P. aeruginosa* (*12*).

Role of Zn^{2+} in LpxC. The role of the required Zn^{2+} in LpxC could be either structural or catalytic in nature. Our data demonstrate that the Zn^{2+} in LpxC is essential for maximal activity but do not unequivocally discriminate between these two possibilities. Loss of either a catalytic or a structural zinc ion may result in similar activity losses upon Zn^{2+} removal; whether this activity loss is due to impaired catalytic function or to loss of structural integrity of the protein must be determined for each enzyme. However, inhibition by the bound hydroxamate compounds (*4*), which readily coordinate Zn^{2+}, suggests that there is an exchangeable site on the Zn^{2+} coordination sphere of LpxC, one hallmark of a catalytic zinc ion.

In the majority of previously studied cases where an enzyme requires a single zinc ion for hydrolysis of an amide bond, such as with the carboxypeptidases, neutral endopeptidases, and angiotensin converting enzyme, the role of that zinc ion is catalytic (*11*, *36*). Some amide-bond-cleaving enzymes, such as *Aeromonas* aminopeptidase and collagenase, contain a second zinc ion, in addition to the catalytic Zn^{2+}, that plays a structural role in enzyme activity (*29*, *37*). However, since stimulation of activity is not observed with the *E. coli* LpxC upon the addition of more than 1 equiv of Co^{2+} (Figure 7A), and since high concentrations of Zn^{2+} are actually inhibitory to LpxC activity (Figures 5 and 6), this is not likely to be the case for this enzyme.

There are several properties of Zn^{2+} that make it particularly useful for this type of catalysis (*38*). Zinc is inert to oxidoreduction, so it can be used to catalyze hydrolytic reactions while avoiding the formation of potentially damaging radical species. Zinc is a strong Lewis acid, yet it retains flexibility in ligand geometry, as it is able to adopt 4-, 5-, or 6-coordinate geometries readily. This characteristic allows a Zn^{2+} metalloenzyme to take advantage of the stability afforded by three protein residues coordinating the active Zn^{2+} while still leaving open one or two sites on the coordination sphere for binding of water molecules or substrates during the reaction.

In general, a number of other metals can substitute for Zn^{2+} in metalloproteins. In carboxypeptidase A (CPA), Co^{2+} and Ni^{2+} are the most efficient replacements for Zn^{2+}, while Mn^{2+}-substituted enzymes exhibit partial activity (*39*, *40*). This pattern of reconstitution likely reflects the strong Lewis acid character of cobalt and nickel (*38*). Co^{2+} is an especially ubiquitous replacement for Zn^{2+} since this metal ion can adopt geometries similar to those preferred by Zn^{2+}, although

Co^{2+} binds preferentially as the 5-coordinated species in proteins (*41*).

The *E. coli* LpxC protein shows a pattern of metal reconstitution similar to CPA. The order of reactivity of the metal-substituted enzymes is $Co^{2+} \sim Ni^{2+} > Zn^{2+} > Mn^{2+}$ (Table 3). Higher activity with the Co^{2+}- or Ni^{2+}-substituted forms of a Zn^{2+} metalloenzyme is not unprecedented; Co^{2+}-CPA is 5 times more active than Zn^{2+}-CPA at catalyzing the hydrolysis of tripeptide substrates (*40*). However, the activity of the Zn^{2+}-substituted LpxC may be underestimated in these experiments due to inhibition by zinc ions (Figures 5 and 6). Reconstitution by Co^{2+} and Ni^{2+} has also been observed at structural Zn^{2+} sites in metalloenzymes. However, in several of these cases, other metals such as Ca^{2+}, Cu^{2+}, or Fe^{2+} are also capable of restoring significant activity to the enzyme (*42*, *43*). This is not the case with LpxC where incubation of the apoenzyme with Ca^{2+}, Cu^{2+}, Cd^{2+}, or Mg^{2+} does not stimulate deacetylase activity. While these results do not constitute definitive proof that the Zn^{2+} in LpxC is catalytic, they are consistent with results for other Zn^{2+} metalloenzymes for which this is the case.

The fact that copper inhibits, rather than activates, purified apo-LpxC is interesting when compared with the results of Hyland and co-workers (*12*), who demonstrated that incubation of EDTA-inactivated extracts of *P. aeruginosa* with Cu^{2+} restored 80% of the deacetylase activity. However, Cu^{2+} binds very tightly both to many Zn^{2+} metalloenzymes, even displacing the native Zn^{2+}, and to EDTA. Therefore, addition of Cu^{2+} to cellular extracts in the presence of EDTA could cause the release of various amounts of Zn^{2+}, thus reconstituting LpxC activity with Zn^{2+} and not Cu^{2+}. In our metal substitution experiments we have limited the potential problem of reconstitution by contaminating Zn^{2+} by using only the purified enzyme in assay systems that are free of other potential sources of contaminating metal, such as BSA or EDTA.

Other Possible Metallodeacetylases. Although LpxC may have mechanistic parallels with the Zn^{2+} proteinases, there is no identifiable sequence similarity between the Zn^{2+} sites in these two classes of enzymes. Metal binding sites of several Zn^{2+} proteinases have been characterized and confirmed by crystallographic data (*13*, *44*). The identity and spatial organization of the Zn^{2+} binding residues are completely conserved among all members of a given family. For the exoproteolytic carboxypeptidases, two protein residues separate two of the metal ligands in an HXXE sequence. Likewise, the neutral endopeptidases, such as thermolysin, have two His ligands separated by three amino acids in an HEXXH motif. One deacetylating enzyme, the acetylpolyamine amidohydrolase from *Mycoplana ramosa*, has a putative Zn^{2+} binding site including the HXXE sequence from the carboxypeptidase family (*45*). However, neither this sequence nor the HEXXH sequence from neutral endopeptidases is found in the amino acid sequence of LpxC from any species (*12*). It is interesting to note that some other deacetylating enzymes are also inhibited by hydroxamate-containing molecules, such as the histone deacetylases that are strongly inhibited by the natural product trichostatin, suggesting that they may contain a catalytic Zn^{2+} site (*46*, *47*). The yeast histone deacetylase (HDA) complex is also inhibited significantly by Zn^{2+}, similar to *E. coli* LpxC (*48*). However, the HXXE and HEXXH Zn^{2+} binding motifs are also absent in the sequences of two histone deacetylases, the mammalian HDA1 protein and its yeast transcriptional regulating homologue Rpd3p (*49*). Additionally, the N^8-acetylspermidine deacetylase is inhibited by both metal-chelating reagents and hydroxamate compounds, suggesting that it may also contain a required zinc ion (*50*). The lack of an identifiable Zn^{2+} binding motif in histone deacetylase and LpxC indicates that these deacetylating enzymes may be part of a previously undescribed family of enzymes that require Zn^{2+} for activity, but do not have a typical metalloproteinase Zn^{2+} binding site.

ACKNOWLEDGMENT

We gratefully acknowledge the assistance of Dr. Yasuhiko Nozaki with performing the dry weight analysis of LpxC and Dr. Matt Anderson for providing us with the LpxC plasmid, pET11a-EnvA. Also, we thank Sharon M. Crary and Timna J. O. Wyckoff for helpful discussions during the preparation of the manuscript.

REFERENCES

1. Raetz, C. R. H. (1993) *J. Bacteriol. 175*, 5745−5753.
2. Raetz, C. R. H. (1996) in *Escherichia coli and Salmonella: Cellular and Molecular Biology* (Neidhardt, F. C., Ed.) pp 1035−1063, ASM Press, Materials Park, OH.
3. Wyckoff, T. J. O., Raetz, C. R. H., and Jackman, J. E. (1998) *Trends Microbiol. 6*, 154−159.
4. Onishi, H. R., Pelak, B. A., Gerckens, L. S., Silver, L. L., Kahan, F. M., Chen, M. H., Patchett, A. A., Stachula, S. S., Anderson, M. S., and Raetz, C. R. H. (1996) *Science 274*, 980−982.
5. Anderson, M. S., Robertson, A. D., Macher, I., and Raetz, C. R. H. (1988) *Biochemistry 27*, 1908−1917.
6. Young, K., Silver, L. L., Bramhill, D., Cameron, P., Eveland, S. S., Raetz, C. R. H., Hyland, S. A., and Anderson, M. S. (1995) *J. Biol. Chem. 270*, 30384−30391.
7. Anderson, M. S., Bull, H. G., Galloway, S. M., Kelly, T. M., Mohan, S., Radika, K., and Raetz, C. R. H. (1993) *J. Biol. Chem. 268*, 19858−19865.
8. Nishino, N., and Powers, J. C. (1978) *Biochemistry 17*, 2846−2850.
9. Harris, R. B., Strong, P. D. M., and Wilson, I. B. (1983) *Biochem. Biophys. Res. Commun. 116*, 394−399.
10. Holmes, M. A., and Matthews, B. W. (1981) *Biochemistry 20*, 6912−6920.
11. Matthews, B. W. (1988) *Acc. Chem. Res. 21*, 333−340.
12. Hyland, S. A., Eveland, S. S., and Anderson, M. S. (1997) *J. Bacteriol. 179*, 2029−2037.
13. Vallee, B. L., and Auld, D. S. (1990) *Proc. Natl. Acad. Sci. U.S.A. 87*, 220−224.
14. Auld, D. S., and Vallee, B. L. (1970) *Biochemistry 9*, 4352−4359.
15. Auld, D. S., and Vallee, B. L. (1970) *Biochemistry 9*, 602−609.
16. Studier, F. W., Rosenberg, A. H., Dunn, J. J., and Dubendorf, J. W. (1990) *Methods Enzymol. 185*, 60−89.
17. Nair, S. K., Calderone, T. L., Christianson, D. W., and Fierke, C. A. (1991) *J. Biol. Chem. 266*, 17320−17325.
18. Laemmli, U. K. (1970) *Nature 227*, 680−685.
19. Kiefer, L. L., and Fierke, C. A. (1994) *Biochemistry 33*, 15233−15240.
20. Hunt, J. B., Neece, S. H., and Ginsburg, A. (1985) *Anal. Biochem. 146*, 150−157.
21. Kelly, T. M., Stachula, S. A., Raetz, C. R. H., and Anderson, M. S. (1993) *J. Biol. Chem. 268*, 19866−19874.
22. Sorensen, P. G., Lutkenhaus, J., Young, K., Eveland, S. S., Anderson, M. S., and Raetz, C. R. H. (1996) *J. Biol. Chem. 271*, 25898−25905.

23. Ferscht, A. (1985) *Enzyme Structure and Mechanism*, 2nd ed.; ed., W. H. Freeman and Company, New York.
24. Jordan, S. P., Zugay, J., Darke, P. L., and Kuo, L. C. (1992) *J. Biol. Chem. 267*, 20028−20032.
25. Gonzalez-Villasenor, L. I., and Powers, D. A. (1985) *J. Biol. Chem. 260*, 9106−9113.
26. Masuoka, J., Hegenauer, J., VanDyke, B. R., and Saltman, P. (1993) *J. Biol. Chem. 268*, 21533−21537.
27. Wetterhom, A., Macchia, L., and Haeggstrom, J. Z. (1994) *Arch. Biochem. Biophys. 311*, 263−271.
28. Larsen, K. S., and Auld, D. S. (1989) *Biochemistry 28*, 9620−9625.
29. Prescott, J. M., Wagner, F. W., Holmquist, B., and Vallee, B. L. (1985) *Biochemistry 24*, 5350−5356.
30. Bertini, I., and Luchinat, C. (1984) *Adv. Inorg. Biochem. 6*, 71−111.
31. Bertini, I., and Luchinat, C. (1983) *Acc. Chem. Res. 16*, 272−279.
32. Young, K., Silver, L. L., Bramhill, D., Caceres, C. A., Stachula, S. A., Shelly, S. E., Raetz, C. R. H., and Anderson, M. S. (1993) *FASEB J. 7*, A1268.
33. Coombs, T. L., Felber, J.-P., and Vallee, B. L. (1962) *Biochemistry 1*, 899−905.
34. Auld, D. S. (1988) *Methods Enzymol. 158*, 110−114.
35. Kidani, Y., and Hirose, J. (1977) *J. Biochem. 81*, 1383−1391.
36. Christianson, D. W., and Lipscomb, W. N. (1989) *Acc. Chem. Res. 22*, 62−69.
37. Lovejoy, B., Cleasby, A., Hassell, A. M., Longley, K., Luther, M. A., Weigl, D., McGeehan, G., McElroy, A. B., Drewry, D., Lambert, M. H., and Jordan, S. R. (1994) *Science 263*, 375−377.
38. Williams, R. J. P. (1995) *Eur. J. Biochem. 234*, 363−381.
39. Peterson, L. M., Sokolovsky, M., and Vallee, B. L. (1976) *Biochemistry 15*, 2501−2508.
40. Auld, D. S., and Holmquist, B. (1974) *Biochemistry 13*, 4355−4361.
41. Jernigan, R., Raghunathan, G., and Bahar, I. (1994) *Curr. Opin. Struct. Biol. 4*, 256−263.
42. Suoranta, K., and Londesborough, J. (1984) *J. Biol. Chem. 259*, 6964−6971.
43. Callahan, S. M., Cornell, N. W., and Dunlap, P. V. (1995) *J. Biol. Chem. 270*, 17627−17632.
44. Vallee, B. L., and Auld, D. S. (1990) *Biochemistry 29*, 5647−5659.
45. Sakurada, K., Ohta, T., Fujishiro, K., Hasegawa, M., and Aisaka, K. (1996) *J. Bacteriol. 178*, 5781−5786.
46. Sanchez del Pino, M. M., Lopez-Rodas, G., Sendra, R., and Tordera, V. (1994) *Biochem J. 303*, 723−729.
47. Yoshida, M., Horinouchi, S., and Beppu, T. (1995) *BioEssays 17*, 423−430.
48. Carmen, A. A., Rundlett, S. E., and Grunstein, M. (1996) *J. Biol. Chem. 271*, 15837−15844.
49. Taunton, J., Hassig, C. A., and Schreiber, S. L. (1996) *Science 272*, 408−411.
50. Huang, T. L., Dredar, S. A., Manneh, V. A., Blankenship, J. W., and Fries, D. S. (1992) *J. Med. Chem. 35*, 2414−2418.

BI982339S